JEE Journal of Ecological Engineering

Journal of Ecological Engineering 2024, 25(7), 384–397
https://doi.org/10.12911/22998993/188917
ISSN 2299–8993, License CC-BY 4.0

Received: 2024.04.07
Accepted: 2024.05.20
Published: 2024.06.01

Optimal Design of a Hybrid Renewable Power System for a Reverse Osmosis Desalination Plant in Jordan

Sara N. Ababneh[1], Mohammad Al-Odat[2*]

[1] Water and Environment Engineering Department, Al-Huson University College, Al-Balqa Applied University, P.O.B. 50, Irbid, Jordan

[2] Mechanical Engineering Department, Al-Huson University College, Al-Balqa Applied University, P.O.B. 50, Irbid, Jordan

* Corresponding author's e-mail: m_alodat@yahoo.com

ABSTRACT

The aim of this investigation is to assess the feasibility and benefits of integrating a renewable energy system into a seawater reverse osmosis (SWRO) desalination station in Aqaba, Jordan. It has been determined that the optimal SWRO system configuration produce 109,500.00 m^3 daily fresh-water output with high rejection rates for various contaminants. The total water cost is 0.85 $/$m^3$, with a specific energy consumption of 2.67 kWh/m^3. Furthermore, the economic and environmental assessments of optimum design of the wind-diesel generator-battery. This configuration not only offers the lowest cost of energy but also demonstrates a substantial renewable fraction and significant reduction in CO_2 emissions. These results underscore the feasibility and benefits of integrating renewable energy into desalination operations, contributing to both economic sustainability and environmental preservation.

Keywords: water desalination, reverse osmosis, hybrid renewable,.

INTRODUCTION

Freshwater availability has emerged as a critical global concern, with less than 3% of Earth's water resources being fresh. The majority of these freshwater resources exist in glaciers, predominantly located in the polar regions, leaving only 0.36% available for exploitation. Climate change and population growth are anticipated to exacerbate freshwater scarcity, making it a pivotal factor in future development. The interdependence of water and energy is evident, as energy is essential for desalination processes, thus an impending water crisis is likely to trigger an energy crisis. Governments are adopting various strategies to mitigate water stress, including dam construction, cloud seeding, desalination, wastewater reuse, and large-scale water transfer projects. Against this backdrop, the prospect of addressing water scarcity through seawater desalination is gaining traction. The unequal distribution of water resources and persistent water scarcity in Jordan pose significant challenges to water resource management (Salameh *et al*., 2021). Despite the limited availability of water, certain areas, particularly urban center, exhibit high rates of water consumption. This unequal distribution has led to the overexploitation of groundwater, resulting in aquifer depletion and exacerbating long-term water scarcity (Alfarra, 2019; Al Omari, 2020; Borgomeo *et al*., 2020). Climate change compounds these issues, with rising temperatures, reduced precipitation, and increased evaporation rates collectively diminishing water availability and worsening water scarcity. Climate change is also expected to heighten the frequency and intensity of droughts and floods, further impacting water resources (Abdulkadir *et al*., 2022; Qtaishat *et al*., 2022). Therefore, desalination is a vital process for conserving water and preserving water resources, particularly in Jordan. Jordan relies on four primary water resources to meet its water needs sustainably: surface water, groundwater, desalinated water, and treated wastewater.

Groundwater and surface water primarily constitute the freshwater resources in the country. Additionally, desalinated water and treated wastewater play significant roles as nonconventional resources, particularly in addressing the gap between water supply and demand, notably in municipal and agricultural sectors. The various available water resources in Jordan encompasses the following components. Also, Jordan faces significant challenges related to its water resources, driven by a combination of population growth, the influx of refugees (Department of Statistics, 2021, World Population Prospects, 2021), and the scarcity of water. In the Middle East and North Africa (MENA), water scarcity is a major concern, with the region being one of the driest in the world. In recent years, a growing body of research has focused on harnessing renewable energy sources for powering desalination plants, particularly in arid regions like Egypt and Jordan, where water scarcity is a pressing issue. Several studies have explored the feasibility and economic viability of different configurations of hybrid renewable energy systems to meet the energy demands of Al-Qawabah *et al*. (2021) investigated renewable power sources for a 100 m^3 per day RO desalination plant near Sail Elhasaa, Jordan. They used the HOMER Hybrid Optimization Model Tool to evaluate different designs, including photovoltaic (PV) systems, wind turbines, diesel generators, and hybrid systems. They found that a hybrid system combining photovoltaic modules with a wind turbine, diesel generator, and Direct Current/ Alternating Current (DC/AC) converter was the most cost-effective solution.

Al-Dhaifallah *et al*. (2023) conducted a study with the aim of harnessing renewable energy systems to power the Tarek Dehays aqua treat seawater reverse osmosis (SWRO) desalination station located adjacent to the Jordan phosphate mines company (JPMC) in Aqaba, Jordan. Twelve power system configurations were investigated and analyzed based on economic and environmental criteria, including diesel generators, batteries, wind turbines, photovoltaic arrays, and fuel cells. The optimal hybrid power system configuration identified is PV-wind-diesel generator-battery, with the lowest cost of energy (COE) at 0.063 $/kWh, a renewable fraction (RF) of 98.2%, and CO_2 emissions totaling 417,752 kg/year. The second-best option is the wind-diesel generator-battery hybrid system, with similar COE and RF but slightly higher CO_2 emissions. The cycle dispatch strategy was favored for its lower net present cost (NPC) and COE compared to the load following strategy, despite resulting in lower RF and higher greenhouse gas emissions. Specifically, the PV-wind-diesel generator-battery system, under the cycle charging strategy, exhibits an NPC of $11,086,499, COE of 0.063 $/kWh, RF of 98.2%, and CO_2 15 emissions of 417,752 kg/year. Conversely, under the load following strategy, it demonstrates an NPC of $11,966,178, COE of 0.068 $/kWh, RF of 99.2%, and CO_2 emissions of 272,335 kg/year.

Alghassab *et al*. (2020) conducted a thorough feasibility and techno-economic assessment near the Jordan borders in NEOM City, Saudi Arabia. The study focused on evaluating various scenarios for a self-sufficient hybrid renewable energy system aimed at powering an eco-friendly seawater desalination plant. The plant produces 150 m^3 of freshwater per day, enough to supply 1000 people. Using HOMER® software, the optimal configuration was determined based on techno-economic analysis and environmental considerations, measured by net present cost and cost of energy. The best configuration was found to be photovoltaic /fuel cell /battery system, with an optimal size of 235 kW PV array, 30 kW FC, 144 batteries, 30 kW converter, 130 kW electrolyzer, and 25 kg hydrogen tank. This setup was considered the most cost-effective, with an NPC of $438,657 and a COE of $0.117/kWh.

This study will help to identify the quality of hybrid system, by identifying size optimization of a hybrid wind/PV/diesel power system for reverse osmosis (RO) desalination plant Jordan. That in turn leads to adopting the hybrid system to produce energy for RO desalination It is expected to obtain many positive results that will benefit the water sector in Jordan to solve the water and drink water problem.

METHODOLOGY

Site description and input parameters

The studied RO system was assumed to be installed on Al-Aqaba. Al-Aqaba is a coastal city located in southern Jordan, and is the only coastal city in the country. It is also the largest and most populous city in the Gulf of Aqaba, with a population of 148,398 in 2015. Al-Aqaba serves as the administrative center of the Aqaba Governorate

and has a land area of 375 square kilometres (144.8 square miles). The city's coordinates are 29.5321° N, 35.0063° E. as shown in Figure 1.

In 2020, Aqaba city in Jordan experienced varying levels of daily irradiance and solar clearance index, as depicted in Figure 2. The average hourly accumulated daily irradiance for the year was recorded at 9.1 kWh/m^2/day. Throughout the year, the minimum and maximum values of daily average solar accumulation were 5.8 kWh/m^2/day and 12.0 kWh/m^2/day, observed in January and June, respectively. In terms of wind conditions, Aqaba city experienced an average wind speed of 9.5 m/s throughout 2020, as depicted in the provided figures. This data indicates favourable conditions for installing wind turbines in the area. The chemical constituents of seawater surrounding Aqaba, are detailed in Table 1 (Al-Taani, *et al*., 2020; WHO, 2011).

Reverse osmosis design

In the investigated desalination system, two cases studied: Case A single-pass seawater reverse osmosis systems and the Case B was two pass split partial (TPSP) SWRO systems. Case A are designed to generate desalinated seawater (permeate) in a single process, utilizing a solitary set of RO trains operating concurrently. Typically, a single-stage SWRO system requires approximately 800 to 900 SWRO membrane elements

Figure 1. Locations of the study areas on the map of Jordan

Table 1. Quality of the Aqaba Feed water

Ion (mg/l)	Raw water	Ion (mg/l)	Raw water
CA^{2+}	452.13	K^{+}	594.08
MG^{2+}	2298.01	NH_4^{+}	14.98
NA^{+}	10801.44	Sr	9.860
CO_3^{2-}	29.93	NO_3^{-}	13.85
HCO_3^{-}	142.20	PO_4^{3-}	0.21
SO_4^{2-}	385.77	OH^{-}	0.20
CL^{-}	24326.40	B (WHO ,2011)	5.30
F^{-}	0.90	CO_2	0.39
NH_3	1.48	pH	8.26
TDS		39075.06	

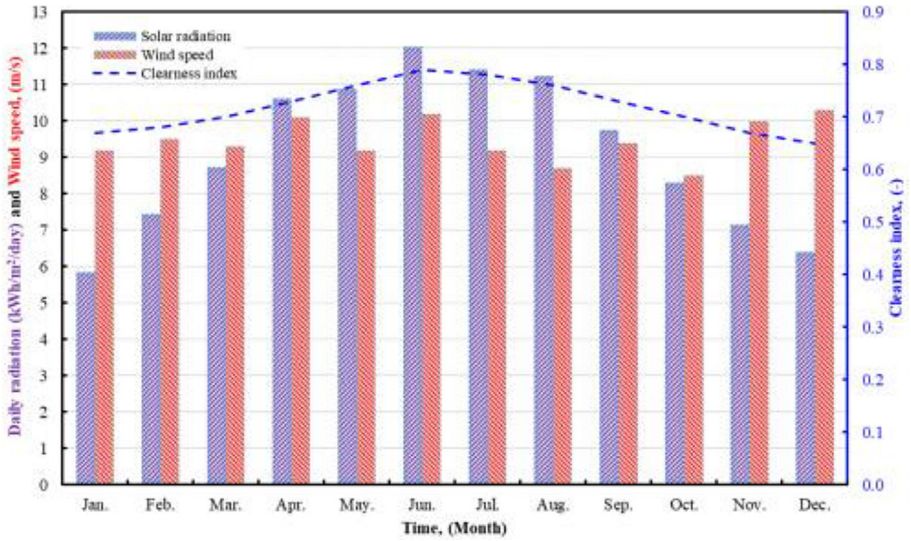

Figure 2. Monthly average daily solar radiation and wind speed at Aqaba

housed within 100 to 150 vessels to produce 10,000 m^3/day (2.6 million gallons per day) of permeate suitable for potable use (Voutchkov, 2013) depicted in Figure 3. Sea water composite (SWC4) MAX elements were utilized in this case. These membranes are renowned for their exceptional salt rejection capabilities when treating various seawater salinities,

In case B a split-partial two-pass configuration is employed, where the second pass of RO typically treats only a portion (ranging from 50% to 75%) of the permeate generated by the first pass (Voutchkov, 2013). The remaining low-salinity permeate that is produced by the front (feed) SWRO elements of the initial pass, is blended directly with the permeate produced by the second RO pass. In this configuration, depicted in Figure 4, The initial pass of the desalination system utilizes SWC4 MAX reverse osmosis elements, while energy-saving polyamide (ESPAB) MAX spiral wound elements are employed in the second pass of both stages. Two scenarios were examined to determine the optimal design: Scenario 1, featuring a permeate recovery rate of 43%, and Scenario 2, with a permeate recovery rate of 45%. In Case A, these two scenarios were applied. Additionally, for Case B, different ratios of P1 Permeate to P2 Feed (50%, 55%, 60%,65%,70%, 75%) were selected under both 45% and 43% permeate recovery rates.

Membrane rejection was determined by comparing the concentration of each compound in the permeate to that in the feed water, resulting in a dimensionless ratio by *Equation (1*).

$$Salt\ rejection = 1 - \frac{C_p}{C_F} \quad (1)$$

where: C_p – concentration of a specific component in the permeate (mg/L), C_F – concentration in the feed (mg/L).

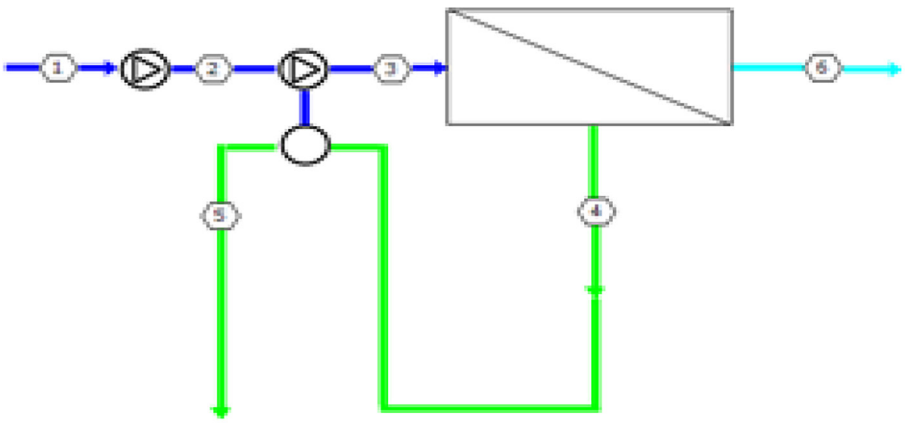

Figure 3. Schematic single-stage diagram of the RO system

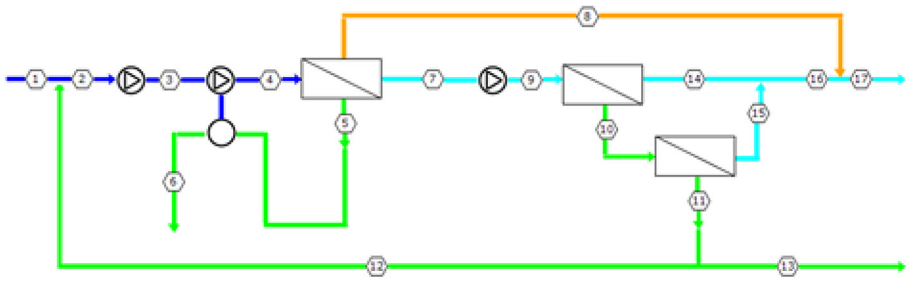

Figure 4. Schematic a TPSP diagram of the RO system

Table 2. Single-stage RO system components configuration scenario 1 and 2

Parameter	Value	
Permeate recovery (%)	43	45
HP pump flow (m^3/h)	1060.93	1013.78
Raw water flow/train (m^3/d)	25465.1	24333.33
Feed pressure (bar)	59.2	60.6
Turbo boost pressure (bar)	25.97 r	25.65
Permeate flow/train (m^3/d)	10950.0	

Table 3. TPSP RO system components configuration permeate recovery 43% in pass 1 and 90% in pass 2

P1 Permeate to P2												
Feed parameter	50%		55%		60%		65%		70%		75%	
	pass 1	pass 2	pass 1	pass 2	pass 1	pass 2	pass 1	pass 2	pass 1	pass 2	pass 1	pass 2
Feed water pH	8.26	6.81	8.26	6.79	8.26	6.77	8.26	6.75	8.26	6.73	8.26	6.70
HP Pump flow (m^3/h)	1060.93	1060.93	1060.93	249.97	1060.93	273.12	1060.93	296.26	1060.93	319.41	1060.93	342.56
Raw water flow/train (m3/d)	24920.7	5444.4	24865.1	6000.0	24809.5	6555.6	24753.9	7111.1	24698.3	7666.7	24642.8	8222.2
Permeate flow/ train (m^3/d)	10950.0	4900.0	10950.0	5400.0	10950.0	5900.0	10950.0	6400.0	10950.0	6900.0	10950.0	7400.0
Feed pressure (bar)	59.5	6.7	59.4	7.4	59.2	8	59.1	8.6	59.0	9.3	58.9	9.9
Turbo boost pressure (bar)	26.02		25.96		25.91		25.86		25.80		25.75	
Total system recovery (%)	43.2		41.6		41.5		41.4		41.2		41.1	

Table 4. TPSP RO system components configuration permeate recovery 45%in pass 1 and 90% in pass 2

P1 Permeate to P2												
Feed parameter	50%		55%		60%		65%		70%		75%	
	pass 1	pass 2	pass 1	pass 2	pass 1	pass 2	pass 1	pass 2	pass 1	pass 2	pass 1	pass 2
Feed water pH	8.26	6.83	8.26	6.81	8.26	6.79	8.26	6.77	8.26	6.74	8.26	6.70
HP Pump flow (m^3/h)	1013.78	226.83	1013.78	249.97	1013.78	273.12	1013.78	296.26	1013.78	319.41	1013.78	342.56
Raw water flow/train (m3/d)	24920.7	5444.4	23733.3	6000.0	23677.7	6555.6	23622.1	7111.1	23566.5	7666.7	23511.0	8222.2
Permeate flow/ train (m^3/d)	10950.0	4900.0	10950.0	5400.0	10950.0	5900.0	10950.0	6400.0	10950.0	6900.0	10950.0	7400.0
Feed pressure (bar)	60.8	6.8	60.7	7.4	60.5	8	60.4	8.7	60.3	9.3	60.1	10
Turbo boost pressure (bar)	25.66		25.61		25.55		25.86		25.44		25.38	
Total system recovery (%)	43.7		43.6		43.5		43.3		43.2		41.1	

The percentage of feed source water flow (Q_f) that is converted to fresh water flow is defined as the permeate recovery rate (Pr) and is calculated from Equation (2). For typical SWRO systems, the recovery rate ranges from 40 to 65% (Voutchkov, 2013).

$$Pr = \frac{Q_p}{Q_F} \times 100\% \quad (2)$$

Membrane permeate flux (J), also known simply as membrane flux, quantifies the volume of permeate produced per unit membrane area using Equation 3. It is determined by dividing the permeate flow rate (Q_p) generated by a RO membrane element (typically measured in gallons per day or liters per hour) by the total membrane area (A) of the element, expressed in square feet or square meters. The flux unit is commonly denoted as gallons per square foot per day (gfd) or liters per square meter per hour (lmh) (Voutchkov, 2013; Aghababaei, 2017).

$$Flux = \frac{Q_p}{A} \quad (3)$$

The concentration polarization factor (CPF or β) expresses an excessive accumulation of dissolved ions at the membrane surface. It is limiting parameter of an RO system design with a shorter combined element length is the CPF and can evaluated by Equation 4 (Voutchkov, 2013).

$$\beta = \frac{C_s}{C_b} \quad (4)$$

where: C_s – salt content at the surface of the membrane (mg/L), C_b – salt content in bulk feed water (mg/L).

This phenomenon results in an increase in salinity within the boundary layer adjacent to the membrane surface, leading to several adverse effects, increased Osmotic Pressure, increased Salt Passage, hydraulic Resistance and scale formation and fouling (Voutchkov, 2013; Aghababaei, 2017). concentration polarization in seawater reverse osmosis systems is influenced by factors such as permeate flux, feed flow rate, and membrane configuration. Increasing permeate flux exacerbates concentration polarization by transporting more salt ions and solids to the boundary layer, while higher feed flow rates may mitigate it by increasing turbulence. Operating at recovery rates above 75% can lead to practical challenges due to high concentration polarization factors, such as scale formation and the need for large quantities of antiscalant. To mitigate concentration polarization, membrane manufacturers recommend maintaining recovery rates per membrane element within 10 to 20 percent. Therefore, a typical SWRO plant is practically limited to 50 to 70% recovery (Voutchkov, 2013).

Energy recovery devices (ERDs) play a vital role in SWRO systems by efficiently recovering high-pressure energy from the concentrate stream. By employing mechanisms such as the Francis turbine, Pelton wheel, and turbocharger, ERDs effectively reduce the energy demands of high-pressure pumps, contributing to the overall efficiency and sustainability of desalination operations (Hernandez *et al*., 2020).

Hybrid renewable energy system components

Photovoltaic array modelling

Photovoltaic systems represent a clean, renewable, and sustainable source of energy production, offering numerous benefits without emitting greenhouse gases. Integration of a PV array into the off-grid hybrid system for powering the reverse osmosis subsystem demonstrates its effectiveness in providing electricity. Through analysis using HOMER software, the PV capacity was determined considering factors such as installation location, panel orientation, and temperature impact, showcasing its viability in decentralized energy solutions. The power output of the PV array in the HOMER software was determined utilizing Equation 5, the PV array rated capacity (kW) ($P_{pv\text{-}rated}$), factor of derating (%) (F_{pv}), the PV array's incident solar radiation (W/m^2) at this moment (GT), radiation at standard test conditions [1 kW/m^2] (Gt, STC), temperature coefficient of power [%/°C] (αp), PV cell temperature in the current time [°C] (Tc), and PV cell temperature under standard test conditions [25 °C] (Tc, STC) (HOMER help manual., Murat, 2018).

$$P_{pv-output} = P_{pv-rated}\, Fpv \left(\frac{Gt}{Gt, STC}\right) \cdot \cdot [1 + \propto p\,(Tc - Tc, STC)] \quad (5)$$

where: $P_{PV\text{-}rated}$ – PV array rated capacity (kW), F_{PV} – derating factor (%), Gt – solar radiation incident on the PV array (W/m^2), $G_{T,STC}$ – radiation at standard test conditions (kW/m^2), αp – temperature coefficient of power (%/°C), Tc – PV cell temperature in the current time [°C], $T_{C,STC}$ – PV cell temperature under standard test conditions (25 °C).

Wind turbines

Wind turbines are converting wind power into electricity, with a wide range of systems available for varying energy demands. The efficiency of wind turbine energy production relies on wind velocity, which is calculated by HOMER software through a meticulous three-step process. This computation accounts for factors like turbine specifications and environmental conditions, ensuring accurate power output estimations for optimal utilization in meeting both production and consumption demands. calculates the wind speed (V_{hub}) at the hub height of the turbine by applying Equation 6. Finally, it adjusts this power output (P_{WT}) value to account for the actual air density (ρ) by Equation 7, where the (HOMER help manual).

$$V_{hub} = V_{anem} \left(\frac{Z_{hub}}{Z_{anem}}\right)^{\propto} \quad (6)$$

$$P_{WT} = \left(\frac{\rho}{\rho 0}\right) P_{WT,STP} \quad (7)$$

where: V_{anem} – wind speed at the height where the measurement at 10 m (m/s), α – the power law exponent, ρ – Actual air density (kg/m^3), ρ_0 – air density at standard temperature and pressure (1.225 kg/m^3).

Inverter

Direct current/alternating current (DC/AC) inverters play a critical role in hybrid systems integrating renewable energy sources like solar PV cells and fuel cells with seawater desalination plants. Their function of converting DC power from renewables to AC power improves system efficiency, ensuring compatibility with the desalination process. Research indicates that the use of DC/AC inverters enhances overall system performance, highlighting their essential role in facilitating efficient power supply to RO desalination plants. Additionally, HOMER's auto-size mode aids in determining optimal converter capacity for these hybrid systems. (Journal of Renewable and Sustainable Energy, 2018).

Battery system

Battery systems are essential for storing excess energy in renewable energy systems, especially in areas without utility connections. While lead-acid batteries are commonly used, they face limitations such as short lifespan and environmental concerns. The selection of an appropriate battery type is crucial, considering factors like charge/discharge cycles and self-discharge rates. Proper sizing of battery banks is necessary based on energy consumption requirements and operational conditions, ensuring optimal performance in hybrid renewable energy systems (Zoulias and Lymberopoulos, 2015)

Diesel generator

Integrating diesel generators into hybrid power systems ensures continuous energy supply, particularly during periods of low renewable energy output or battery depletion. The fuel consumption rate of diesel generators, correlates with their electrical output, influencing system reliability and operational costs. Properly configured diesel generators serve as reliable backup power sources, enhancing the overall resilience and performance of hybrid energy production systems (Mohammed et al., 2015, HOMER help manual). The fuel consumption rate (L/h) of the diesel generator can be determined using Equation 8 ,which correlates with its electrical output. Typical values for Fuel curve intercept coefficient (F_0) and Fuel curve slope (F_1) are = 0.246 L/kWh and F1 = 0.08145 L/kWh respectively, Electrical output of the generator (P_G) and Rated capacity of the generator (P_R)which were used in this study (HOMER help manual).

$$FC_{DG} = F_0 \times P_G + F_1 \times P_R \quad (8)$$

where: F_0 – fuel curve intercept coefficient (h/kW), F_1 – fuel curve slope (h/kW), P_G – electrical output of the generator (kW).

Various scenarios were explored to determine the optimal configurations, based on the net present cost and the cost of energy. The NPC is computed considering capital expenses, replacement costs, and operational and maintenance (O&M) expenses over the projected lifespan, along with salvage value. as described by the following Equation (9) and capital recovery factor (CRF) can be calculated using Equation 10, where n is lifetime of the proposed hybrid system , lifetime of the hybrid system (t) and C_{total} is total annual cost (HOMER help manual, Murat, 2018; Alghassab et al., 2020).

$$NPC = \frac{C_{total}}{CRF\ (i,t)} \quad (9)$$

$$CRF = \frac{i(1+i)^n}{(1+i)-1} \quad (10)$$

where: C_{total} – total annual cost ($/year), i – annual discount rate (%), t – lifetime of the

hybrid system, n – lifetime of the proposed hybrid system (years) which is assumed to be 20 years.

In HOMER, the real discount rate and discount factors were used to calculate the annualised costs from the net present costs. The real discount rate (i) is calculated using the following formula Equation (11) (HOMER help manual, Murat, 2018; Alghassab *et al*., 2020).

$$i = \frac{i'-f}{1+f} \tag{11}$$

where: i' – nominal discount rate, f – expected inflation rate.

The discount rate and inflation rate in this study were considered to be 3% and 2%, respectively) (HOMER help manual; Murat, 2018; Alghassab *et al*., 2020). The simulation incorporates technical and economic specifications of the power system listed in Table 5.

RESULT AND DISCUSSION

The optimal reverse osmosis configuration is achieved with a permeate recovery of 43%. This setting results in lower specific energy consumption compared to a 45% recovery rate. Additionally, it maintains a lower total dissolved solids (TDS) concentration in the concentrate, reducing the risk of fouling and operational challenges. Overall, a 43% permeate recovery balances energy efficiency, operational stability, and

Table 5. The techno-economic data for the power system considered

Energy System	Parameter	Value
PV unit	Capital cost [$ per kW]	3,000.00
	Operation and maintenance [$ per year]	10
	Lifetime [years]	25
	Derating factor [%]	96
	Ground reflection [%]	20
Wind turbine system	Capital cost [$ per unit]	3,000,000.00
	Operation and maintenance cost [$ per year]	30,000.00
	Rated power [kW]	1500
	Lifetime [years]	20
	Hub height [m]	80
Diesel gen-set	Capital cost [$ per kW]	$300.00
Generic large genset	Replacement cost [$ per kW]	$300.00
	Lifetime [hours]	15,000.00
	Operation and maintenance [$ per hour]	$0.010
	Diesel fuel price [$ per L]	1
Batteries	Nominal voltage [V]	600
(Generic 1 kWh Lead Acid)	Nominal capacity [kWh]	1
	Maximum capacity [Ah]	1.6
	Roundtrip efficiency [%]	90
	Maximum charge current [A]	1.67
	Minimum state of charge [%]	20
	Cost [$ per unit]	700,000.00
	Operation and maintenance [$ per year]	10,000.00
	Replacement cost [$ per unit]	700,000.00
	Lifetime [years]	15
Converter	Capital cost [$ per kW]	300
	Replacement cost [$ per kW]	300
	Operation and maintenance [$ per year]	0
	Lifetime [years]	15
	Efficiency [%]	95

cost-effectiveness, making it the preferred choice for the RO system.

Table 6 and Table 7, present the values for specific energy (kWh/m^3), water cost ($/m^3), total product (m^3/d), and total dissolved solids concentration in the concentrate for the TPSP configuration at permeate recoveries of 45% and 43%, respectively. In the TPSP configuration, extensive evaluation across various permeate recoveries and P1 Permeate to P2 Feed ratios demonstrated nuanced differences in performance metrics. At 45% permeate recovery, the 50% P1 Permeate to P2 Feed ratio showcased the lowest specific energy consumption (2.96 kWh/m^3) and the highest total product output (104056 m^3/d). Despite a slightly higher TDS concentration in the concentrate compared to the 75% ratio, the 50% ratio offered superior energy efficiency and productivity, with a marginal trade-off in TDS concentration. Similarly, at 43% permeate recovery, the 50% ratio exhibited the most favorable outcomes, mirroring the trends observed at 45% recovery but with slightly improved specific energy consumption (2.95 kWh/m^3) and total product output (104056 m^3/d). The consistent superiority of the 50% ratio underscores its robustness across different permeate recovery rates, making it the recommended choice for optimizing the TPSP configuration's performance. Additionally, comparing the single-pass configuration at 43% and 45% permeate recoveries, the 43% recovery scenario consistently showed advantages in specific energy consumption and TDS concentration in the concentrate. This reaffirms the preference for a 43% permeate recovery in the single-pass configuration, ensuring both energy efficiency and water quality considerations are met effectively. Therefore, careful consideration of both permeate recovery rates and P1 Permeate to P2 Feed ratios is essential for achieving optimal performance and cost-effectiveness in RO systems. Figure 5 and Figure 6 show the specific energy (kWh/m^3) and The TDS concentration in the concentrate (mg/L) for the TPSP configuration at permeate recoveries of 43% and 45%.

After evaluating Table 9 data, the single-stage SWRO setup with 43% permeate recovery proved most efficient, showcasing a 9.4% energy saving and 12.37% lower water cost compared to TPSP. Despite a 5.23% increase in total permeate production with the single-stage, there was

Table 6. The values for specific energy (kWh/m^3), water cost ($/m^3), total product (m^3/d), and total dissolved solids concentration in the concentrate for the single-stage configuration

Permeate recovery	45%	43%
Specific energy (kWh/m^3)	2.69	2.67
Water cost ($/m^3)	0.85	0.85
Total product (m^3/d)	109500	109500
Concentrate (mg/L)	70867.59	68384.07

Table 7. The values for specific energy (kWh/m^3), water cost ($/m^3), total product (m^3/d), and total dissolved solids concentration in the concentrate for the TPSP configuration at permeate recoveries of 45%

P1 Permeate to P2 Feed	50%	55%	60%	65%	70%	75%
Permeate recovery	45%	45%	45%	45%	45%	45%
Specific energy (kWh/m^3)	2.96	3	3.04	3.08	3.12	3.17
Water cost ($/m^3)	0.97	0.97	0.97	0.97	0.97	0.98
Total product (m^3/d)	104056	103500	102944	102389	101833	101278
Concentrate (mg/L)	69405.02	69250.13	69093.5	68935.37	68775.73	68617.08

Table 8. The values for specific energy (kWh/m^3), water cost ($/m^3), total product (m^3/d), and total dissolved solids concentration in the concentrate for the TPSP configuration at permeate recoveries of 43%

P1 Permeate to P2 Feed	50%	55%	60%	65%	70%	75%
Permeate recovery	43%	43%	43%	43%	43%	43%
Specific energy (kWh/m^3)	2.95	2.99	3.03	3.07	3.12	3.16
Water cost ($/m^3)	0.97	0.97	0.97	0.97	0.97	0.98
Total product (m^3/d)	104056	103500	102944	102389	101833	101278
Concentrate (mg/L)	67032.18	66887.79	66743.91	66598.6	66451.77	66306.16

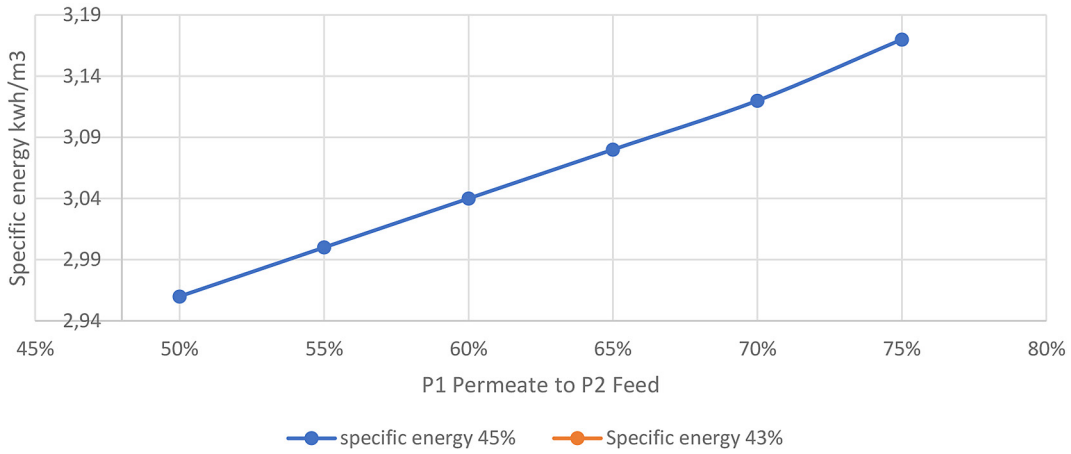

Figure 5. The specific energy (kWh/m^3) for the TPSP configuration at permeate recoveries of 43% and 45%

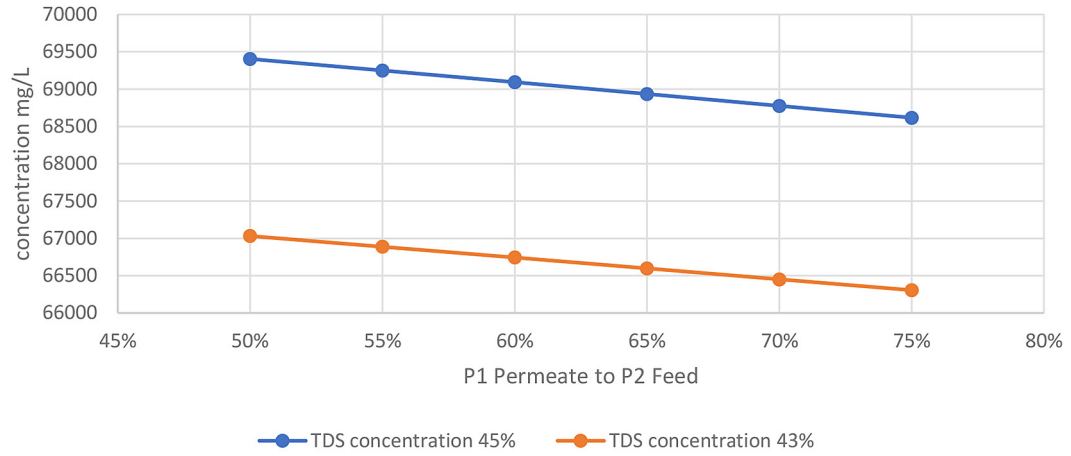

Figure 6. The TDS concentration in the concentrate (mg/L) for the TPSP configuration at permeate recoveries of 43% and 45%

Table 9. Comparison of SWRO configurations: specific energy consumption, total water cost, and permeate production

Configuration	Specific energy consumption(kwh/m^3)	Total water cost (USD/m^3)	Total permeate production (m^3/d)	TDS concentration in the concentrate (mg/L)
Single stage	2.67	0.85	109500.00	68384.07
TPSP	2.95	0.97	104056	67032.18

a slight 2.01% rise in TDS concentration in the concentrate. Overall, the single-stage design offers significant energy and cost benefits with minor trade-offs in TDS concentration.

The single-stage reverse osmosis configuration at a pressure of 59.2 bar, as detailed in Table 10, demonstrates efficient removal of various ions from the permeate water. Notably, it achieves high rejection rates, with 99.88% for sulfate (SO_4^{2-}), 99.55% for total dissolved solids, 99.527% for chloride (Cl^-), 85.92% for boron (B), and 99.33% for sodium (Na^+). Additionally, the TDS level falls within acceptable limits, but it's important to note that water becomes increasingly unpalatable as TDS levels exceed around 1000 mg/L (WHO, 2011).

In the study, specific energy consumption of the RO system was found to be 2.67 kWh/m^3, to produce daily fresh water capacity of 109500 m^3. Through detailed modelling and optimization using HOMER software, an optimal hybrid power system combining wind, and diesel generators with battery backup was identified, the schematic diagram for optimum design shown in Figure 7. This solution, spanning a project life of up to 25

Table 10. Ion concentrations in permeate water from single-stage reverse osmosis systems, with World Health Organization recommendations and Jordanian Standards

Ion (mg/l)	Permeate water (single-stage)	WHO recommendation (mg/L)	Jordanian Standards (mg/L)
Ca^{2+}	0.031	100	200
Mg^{2+}	0.160	50	150
Na^{+}	72.085	200	200
K^{+}	4.943	12	20
NH_4^{+}	0.149	1.5	0.2
Sr	0.007	-	0.2
CO_3^{2-}	1.209	-	-
HCO_3^{-}	0.457	-	500
SO_4^{-2}	115.053	250	500
Cl^{-}	0.009	250	500
F^{-}	0.488	1.5	1.5
NO_3^{-}	0.000	50	50
PO_4^{-3}	0.001	0.05	-
OH^{-}	0.746	-	-
B	0.39	2.4	2.4
CO_2	1.48	-	-
NH_3	195.34	1	-
TDS	6.68	500	1000
pH	0.031	6.5–8.5	6.5–8.5

years, prioritizes low NPC values and renewable energy fractions, showcasing a sustainable approach to water desalination with minimized operational costs. Figure *8* shows the NPC results of the optimised simulations. The battery has maximum NPC with 210,458,298.08 $ following by wind turbine (WT), diesel generator (DG) with 183,434,241.58 $ and 165,873085.13 $ respectively, the system converter has the lowest value with 9,133,869.16 $. The diesel generator system used for sustainability of electricity production for an RO system. According to simulation results, this case had the lowest capital cost ($527 M). In this study, it was assumed that the diesel fuel price was $1.0/L in Aqaba, Jordan. As clearly shown in Figure 9 the total installed cost of that component at the beginning of the project was $270,899,142.99. Subsequent replacement costs are estimated to reach $114,899,142.99, $126,000,000, and $30,000,000 at the 15th, 20th, and 22nd years respectively. The fuel and operating costs remain constant throughout the plant's lifetime at $5,242,500 and $3,519,000 respectively. A salvage value of $156,677,657.40 is expected at the conclusion of the 25th year. The operating cost is the annualized of all costs and revenues other than initial capital costs was 13.5 $/yr. The levelized cost of energy (LCOE) values across for the optimum solution was 0.241 $/kWh.

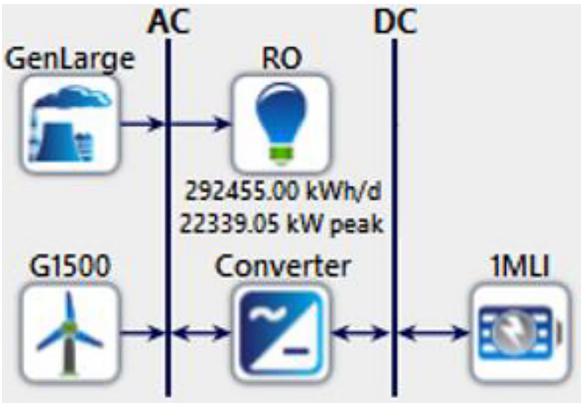

Figure 7. The schematic diagram for optimum design

The optimized configuration consists of 42 wind turbines and 156 batteries, a 100,000 kW diesel generator and 7.35 kW converter. In this scenario, the wind turbine contributes 188,489,952 kWh/y, the diesel generator produces 17,475,000 kWh of electricity with 5,242,500 L fuel consumption operating 699 hours the fuel cost up to 5,242,500 $/y the optimal choice due to its substantial utilization of renewable sources the renewable factor was 83.6% and the resulting

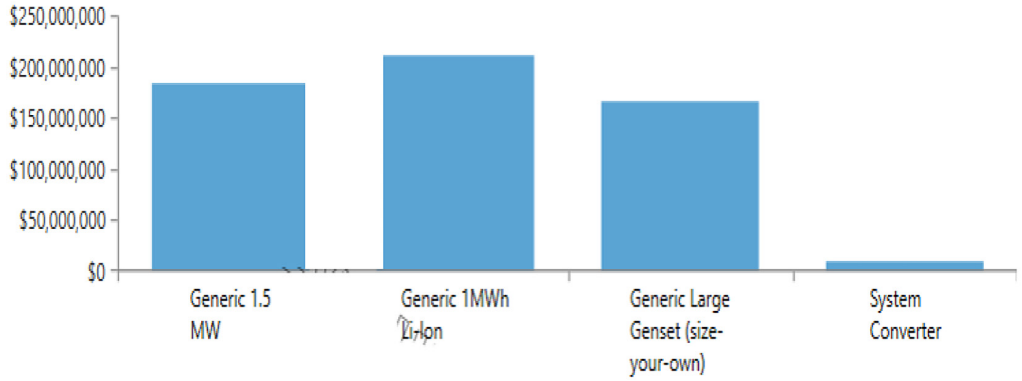

Figure 8. The net present cost by component

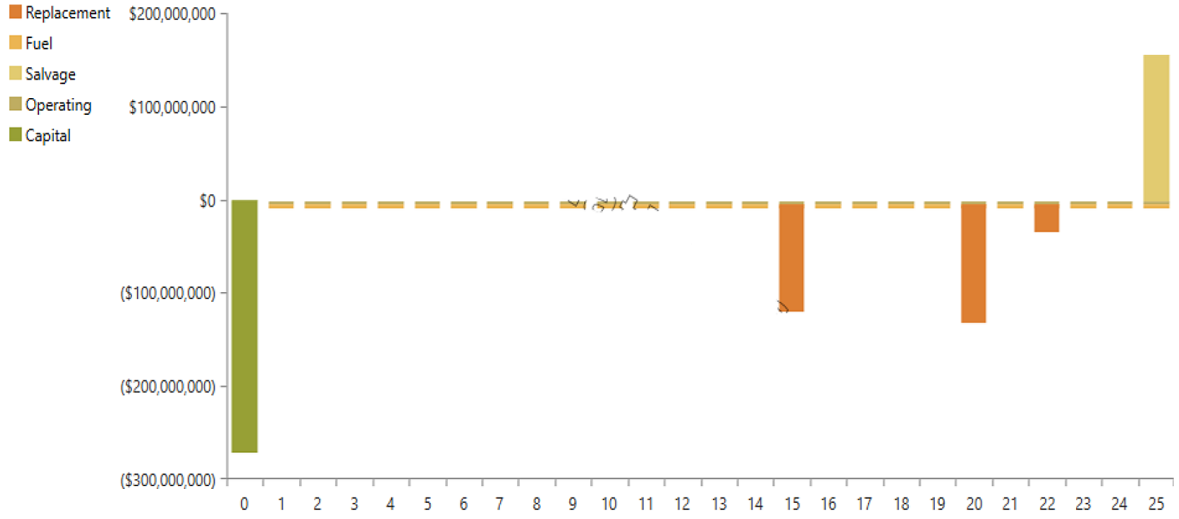

Figure 9. Cash flow summary for the best optimise RES

Table 11. Emissions of pollutants from power generation systems supplemented by diesel generators

Pollutant	Value (kg/y)
Carbon dioxide	13,747,017
Carbon monoxide	71,120
Unburned hydrocarbons	3,775
Particulate matter	608
Sulfur dioxide	33,604
Nitrogen oxides	13,630
Total emission	13,869,754

levelized cost of electricity, standing at $0.241/kWh. The emissions of pollutants for the various scenarios examined in this system are outlined in Table 11. Despite the presence of pollutant emissions in the proposed hybrid configuration, they are notably lower compared to systems relying solely on diesel generators the renewable factor up to 83.6%. It is evident that as the operational hours of the diesel generator within the power system diminish, the emissions of pollutants released into the environment also decrease.Wind

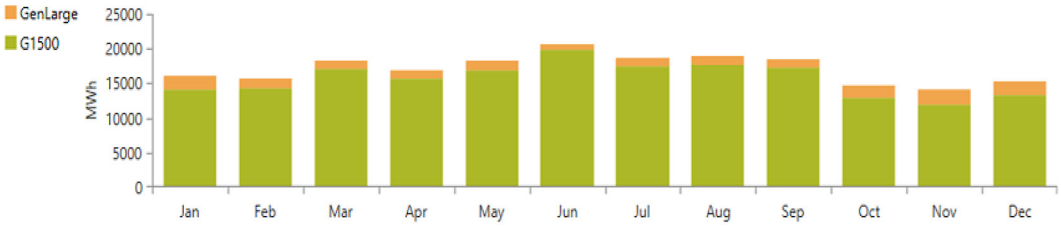

Figure 10. Monthly average electricity production for system

turbines play a significant role in electricity generation due to the high wind speeds at the site, leading to substantial contributions. The monthly average electricity production by wind turbines appears to be similar, with the highest value observed in June, followed by March, July, and August, the contribution of the diesel generator to the power system is minimal due to the presence of renewable sources Figure 10.

CONCLUSIONS

This study systematically assessed various power generation systems (including wind turbine, PV, diesel generator, and battery) suitable for an RO system with a daily capacity of 109500.00 m^3/d on Aqaba, Jordan. The objective was to leverage local energy resources such as solar and wind energy. The analyzed power generation systems encompassed standalone diesel, wind, and PV systems, The technical and economic feasibility of each system was assessed using the HOMER simulation software. From this study, the following conclusions were derived:

- the single-stage configuration offers significant advantages, it achieved energy savings of approximately 9.4% for specific energy consumption and 12.37% for total water cost, additionally, the single-stage configuration demonstrated a notable increase of 5.23% in total permeate production while retaining the same number of trains (10 trains). However, it's important to note that the concentration of total dissolved solids in the concentrate saw a slight increase of 2.01% with this configuration;
- the optimal configuration for the SWRO system involves a single pass arrangement comprising 10 trains, each equipped with 132 vessels. Within each vessel, 7 SWC4 MAX type membranes are utilized. Operating at a permeate recovery rate of 43% and a calculated feed pressure of 59.2 bar;
- the system achieves a daily fresh-water output of 109,500.00 m^3 with a total dissolved solids concentration of 195.34 mg/L. The system exhibits rejection rates of 99.88% for SO_4^{2-}, 99.55% for TDS, 99.527% for Cl^-, 85.92% for B, and 99.33% for Na^+;
- the total water cost is 0.85 \$/m^3, with a specific energy consumption of 2.67 kWh/m^3, the initial investment cost amounts to 10,105,740 USD, with a designed plant life of 15 years;
- the optimised hybrid power system for driving the RO system according to the simulation results was the wind-diesel hybrid system with a battery. which was comprised of 42 wind turbine (10 kW rated capacity), a 100,000 kW diesel generator, a 18,997 kW converter, and 156 strings of 1 MWh LA battery;
- the cost of the electricity generated by the proposed optimised hybrid system was found to be \$0.308/kWh. The NPC and RF values of the optimised hybrid system were \$569 M and 83.6%, respectively;
- the LCOE value for the system was calculated to be 0.241\$/kWh, because of the high cost of the wind turbines;
- the inclusion of renewable resources in a power generation system resulted in minimising the fossil fuel consumption and harmful emissions;
- the carbon dioxide emissions released by this system were 13,747,017 kg/y, it was found that the use of a hybrid power system instead of a diesel generator only reduced the annual CO_2 emissions by 92%.

REFERENCES

1. Al Omari, H. 2020. Water Management in Jordan and its Impact on Water Scarcity (Doctoral dissertation, Université d'Ottawa/University of Ottawa).
2. Alfarra, A. 2019. Water-Energy-Food Nexus in the Arab Region. In Water, Sustainable Development and the Nexus, 74–98. CRC Press.
3. Al-Qawabah, S.M., Al-Soud, M.S., Althneibat, A.K. 2021. Assessment of hybrid renewable energy systems to drive water desalination plant in an arid remote area in Jordan. International Journal of Green Energy, 18(5), 503–511.
4. Al-Taani, A.A., Rashdan, M., Nazzal, Y., Howari, F., Iqbal, J., Al-Rawabdeh, A., Al Bsoul A., Khashashneh, S. 2020. Evaluation of the Gulf of Aqaba coastal water, Jordan. Water, 12(8), 2125.
5. Borgomeo, E., Fawzi, N.A.M., Hall, J.W., Jägerskog, A., Nicol, A., Sadoff, C.W., Salman M., Santos N., Talhami, M. 2020. Tackling the trickle: ensuring sustainable water management in the Arab region. Earth's Future, 8(5), e2020EF001495.
6. Gökçek, M. 2018. Integration of hybrid power (wind-photovoltaic-diesel-battery) and seawater reverse osmosis systems for small-scale desalination applications. Desalination, 435, 210–220.
7. Gomaa, M.R., Ala'a, K., Al-Dhaifallah, M., Rezk, H., Ahmed, M. 2023. Optimal design and economic analysis of a hybrid renewable energy system for

powering and desalinating seawater. Energy Reports, 9, 2473–2493.

8. HOMER help manual., (n.d.). http://www.homerenergy.com/pdf/ HOMERHelpManual.pdf.
9. Aghababaei, N. 2017. Reverse osmosis design with IMS design software to produce drinking water in Bandar Abbas, Iran, Journal of Applied Research in Water and Wastewater, 4(1), 314–318.
10. Qtaishat, T.H., Al-Karablieh, E.K., Al Adaileh, H., El-Habbab, M.S. 2022. Drought Management Policies and Institutional Mandate in Jordan. In Sustainable Energy-Water-Environment Nexus in Deserts: Proceeding of the First International Conference on Sustainable Energy-Water-Environment Nexus in Desert Climates, 757–763. Cham: Springer International Publishing.
11. Rezk, H., Alghassab, M., Ziedan, H.A. 2020. An optimal sizing of stand-alone hybrid PV-fuel cell-battery to desalinate seawater at saudi NEOM city. Processes, 8(4), 382.
12. Salameh, M.T.B., Alraggad, M., Harahsheh, S.T. 2021. The water crisis and the conflict in the Middle East. Sustainable Water Resources Management, 7, 1–14.
13. Schunke, A.J., Hernandez Herrera, G.A., Padhye, L., Berry, T.A. 2020. Energy recovery in SWRO desalination: current status and new possibilities. Frontiers in Sustainable Cities, 2, 9.
14. Sholagberu, A.T., Okikiola, F.O., Bashir, A., Adeniyi, A.S., Juliana, I.O., Muhammad, M.M., Abdurrasheed, A.S. 2022. Performance Evaluation of SWAT-based Model for the Prediction of Potential and Actual Evapotranspiration. Jordan Journal of Civil Engineering, 16(1).
15. UN. World Population Prospects 2019; UN: New York, NY, USA, 2021.
16. Voutchkov, N. 2013. Desalination engineering: planning and design. (No Title).
17. WHO, Guidelines for Drinking-Water Quality, Recommendation., World Health Organization, fourth edition, 2011.
18. Zoulias, E.I., Lymberopoulos, N. 2007. Techno-economic analysis of the integration of hydrogen energy technologies in renewable energy-based stand-alone power systems, Renewable Energy, Elsevier, 32(4), 680–696.